Pflugers Arch - Eur J Physiol (2014) 466:2089–2099
DOI 10.1007/s00424-014-1472-8

ION CHANNELS, RECEPTORS AND TRANSPORTERS

Cinnamaldehyde inhibits L-type calcium channels in mouse ventricular cardiomyocytes and vascular smooth muscle cells

Julio Alvarez-Collazo · Lucía Alonso-Carbajo · Ana I. López-Medina · Yeranddy A. Alpizar · Sendoa Tajada · Bernd Nilius · Thomas Voets · José Ramón López-López · Karel Talavera · María Teresa Pérez-García · Julio L. Alvarez

Received: 23 January 2014 / Revised: 31 January 2014 / Accepted: 4 February 2014 / Published online: 25 February 2014

Abstract Cinnamaldehyde (CA), a major component of cinnamon, is known to have important actions in the cardiovascular system, including vasorelaxation and decrease in blood pressure. Although CA-induced activation of the chemosensory cation channel TRPA1 seems to be involved in these phenomena, it has been shown that genetic ablation of *Trpa1* is insufficient to abolish CA effects. Here, we confirm that CA relaxes rat aortic rings and report that it has negative inotropic and chronotropic effects on isolated mouse hearts. Considering the major role of L-type Ca^{2+} channels in the control of the vascular tone and cardiac contraction, we used whole-cell patch-clamp to test whether CA affects L-type Ca^{2+} currents in mouse ventricular cardiomyocytes (VCM, with Ca^{2+} as charge carrier) and in mesenteric artery smooth muscle cells (VSMC, with Ba^{2+} as charge carrier). We found that CA inhibited L-type currents in both cell types in a concentration-dependent manner, with little voltage-dependent effects. However, CA was more potent in VCM than in VSMC and caused opposite effects on the rate of inactivation. We found these divergences to be at least in part due to the use of different charge carriers. We conclude that CA inhibits L-type Ca^{2+} channels and that this effect may contribute to its vasorelaxing action. Importantly, our results demonstrate that TRPA1 is not a specific target of CA and indicate that the inhibition of voltage-gated Ca^{2+} channels should be taken into account when using CA to probe the pathophysiological roles of TRPA1.

Keywords Blood pressure · Calcium channel · Inotropic effect · Vasorelaxation · TRPA1

Introduction

Cinnamon is a widely popular spice that has been long used in traditional medicine [31] for its alleged antimicrobial, antioxidant, and anti-inflammatory effects [17, 25] and more recently in the treatment of diabetes [3]. Cinnamon is also considered to improve blood circulation [36] and has raised interest for its potential use to decrease blood pressure [1, 2, 23]. Notably, it has been found that the main component of the cinnamon bark, cinnamaldehyde (CA), has important actions in the cardiovascular system.

Early in the 1970s Harada and Yano [20] found that CA (1–10 mg/kg) induces a fast decrease in arterial blood pressure (BP) in anesthetized dogs and guinea pigs, with minor effects on the electrocardiogram. The decrease in BP was attributed to the peripheral vasodilating action of CA. In addition, it was shown that single applications of CA (50–500 μg) to guinea pig-isolated atria and perfused hearts increased contractile force and spontaneous heart rate. However, these effects were transient, and repeated applications led to inhibitory effects. Arrhythmias were observed at the highest CA concentrations used. The action of CA was further investigated by Harada and

Julio Alvarez-Collazo and Lucía Alonso-Carbajo shared first authorship.

J. Alvarez-Collazo · A. I. López-Medina · J. L. Alvarez
Laboratorio de Electrofisiología, Instituto de Cardiología y Cirugía Cardiovascular, Habana, Cuba

L. Alonso-Carbajo · S. Tajada · J. R. López-López · M. T. Pérez-García
Departamento de Bioquímica y Biología Molecular y Fisiología e Instituto de Biología y Genética Molecular (IBGM), Universidad de Valladolid y CSIC, Valladolid, Spain

L. Alonso-Carbajo · Y. A. Alpizar · B. Nilius · T. Voets · K. Talavera (✉)
Laboratory for Ion Channel Research and TRP Research Platform Leuven (TRPLe), Department of Cellular and Molecular Medicine, KU Leuven, Campus Gasthuisberg, O&N1, bus 802. Herestraat 49, 3000 Leuven, Belgium
e-mail: Karel.talavera@med.kuleuven.be

Saito [19], who showed that at high doses (up to 50 mg/kg), it induced an increase in BP that was preceded by a transient fall.

Research on the effects of CA on the cardiovascular system was revived by the finding that it activates the chemosensory cation channel TRPA1 in nociceptive neurons, with high specificity over other sensory transient receptor potential (TRP) channels [6] and by a study proposing that activation of this channel induces vasorelaxation due to a release of calcitonin gene-related peptide (CGRP) from perivascular nerve terminals [7]. Another mechanism by which CA may cause vasodilation is via smooth muscle cell hyperpolarization triggered by activation of endothelial TRPA1 channels located at myoendothelial junction sites [12, 13, 35]. Importantly, CA has been used to probe the role of TRPA1 in vasodilation and axon reflex flare reaction in humans [30] and the vascular function in mice [34]. However, the latter study showed that genetic ablation of *Trpa1* did not abolish the acute reflex changes in blood pressure by systemic CA nor the relaxing action of CA in mesenteric arteries (with or without endothelium).

Interestingly, other studies also suggest for TRPA1-independent actions of CA in the vasculature. For instance, Yanaga et al. demonstrated a concentration-dependent vasorelaxing action of CA on rat aortic rings pre-contracted with prostaglandin $F_{2\alpha}$ or KCl [40]. Although with low potency, CA relaxed aortic rings in the absence of endothelial function. Since CA (0.1–1 mM) significantly shifted the $[Ca^{2+}]$-contraction relationship, it was suggested that CA could exert a direct inhibitory effect on contraction by blocking Ca^{2+} channels. Furthermore, El-Bassossy et al. [14] showed that CA protected from the hypertension associated with diabetes in rats and suggested that the underlying mechanism could be related to a blockade of the increased Ca^{2+} influx to the vascular cells that occurs in this pathology. Finally, Xue et al. [39] demonstrated that CA relaxed rat aortic rings pre-contracted with phenylephrine irrespective of the presence of endothelium and with the same potency and similar effective inhibitory concentration (IC_{50}, ~10 μM). Pretreatment of endothelium-intact aortic rings with L-NAME, ODQ (1H-[1,2,4]-oxadiazole-[4,3-a]-quinoxalin-1-one), or prostaglandin I_2 did not affect CA-induced vasodilatation. This vasorelaxing effect of CA was maintained in endothelium-denuded rings pre-incubated with K^+ channel blockers. However, the vasoconstriction induced by 60 mM K^+ was significantly diminished by CA (~10 μM). The authors concluded that the vasodilatory effect of CA was not mediated by the nitric oxide/cyclic guanosine monophosphate pathway nor by K^+ channels and speculated that CA was most probably affecting Ca^{2+} influx through voltage-gated and receptor-operated Ca^{2+} channels.

This body of evidence and the dominant role of L-type Ca^{2+} ($Ca_V1.2$) channels in the control of the vascular tone and blood pressure regulation [28, 41] and cardiac contraction [8] prompted us to study the effects of CA on the L-type Ca^{2+} currents (I_{CaL}). We first corroborated that CA affects the cardiovascular function, inducing vasorelaxation of rat aortic rings and exerting negative inotropic and chronotropic effects in isolated mouse hearts. Subsequently, we found that CA induces a concentration-dependent and reversible decrease of I_{CaL} in mouse ventricular cardiomyocytes and vascular smooth muscle cells from mesenteric arteries.

Materials and methods

We used male Wistar rats (for aortic ring measurements), male C57BL/6 mice (for Langendorff and VCM patch-clamp), and blood pressure normal (BPN) mice (Jackson Laboratories, Sacramento, USA) (for VSMC patch-clamp). All protocols for animal use were approved by the Institutional Care and Use Committee of the University of Valladolid and were in accordance with the European Community guiding principles in the care and use of animals (86/609/CEE, CE Off J n8L358).

Rat aortic rings

Abdominal aortic rings were dissected from rats under pentobarbital anesthesia. Care was taken to mechanically remove the endothelium by gently rubbing the aorta. They were fixed to a force transducer and placed in a bath chamber continuously perfused (10 ml/min) with the same Tyrode solution used for isolated hearts (pH=7.4, gassed with O_2; T=35 °C) and stabilized, under a load of 0.5 g, for 30 min before the beginning of the experiment. Contraction was induced by replacing NaCl by KCl (60 mM). Absence of endothelium was assessed for all studied rings by acetylcholine (10 μM) application of pre-contracted rings.

Langendorff mouse hearts

As previously described [15], hearts were removed under pentobarbital anesthesia and mounted on a Langendorff column perfused at constant flow (10 ml/min) with a Tyrode solution of the following composition (in mM): NaCl 140, KCl 2.5, $MgCl_2$ 0.5, $CaCl_2$ 2, Tris-hydroxymethylaminomethane 10, and glucose 5 (pH=7.4, gassed with O_2; T=35 °C). A bipolar platinum electrode was placed on the right ventricular epicardium, and the surface electrocardiogram (ECG) was recorded. Another bipolar platinum electrode was placed near the atrioventricular ring and was connected to an SEN-7103 electronic stimulator (Nihon Kohden, Tokyo, Japan). The cardiac apex was fixed to a force-displacement transducer to record the force of contraction (FC). ECG and FC values were recorded at the spontaneous heart rate and at a fixed stimulus rate (400 bpm). Hearts were

let to stabilize for at least 30 min before beginning the experiments.

Isolation of ventricular cardiomyocytes

Male adult mice were anesthetized with pentobarbital (i.p., 0.03 mg/g body weight), and the hearts were quickly removed and placed in cold Ca^{2+}-free Tyrode solution. Ventricular cardiomyocytes were isolated following a procedure previously described [5]. Hearts were quickly removed and placed in cold Ca^{2+}-free Tyrode solution containing (in mM): NaCl 117, KCl 4, KH_2PO_4 1.5, $NaHCO_3$ 4.4, $MgCl_2$ 1.7, HEPES 10, glucose 10, and pH 7.4. After careful dissection, hearts were mounted on a Langendorff column and washed for ~2 min with Tyrode solution containing 0.23 mM EGTA at 35 °C. Hearts were then perfused with Tyrode containing ~100 μM Ca^{2+} and collagenase CLS2 (Worthington, Lakewood, USA) and re-circulated for 7–10 min. After this period, the tissue was cut into small pieces and gently agitated for 2–3 min in fresh enzyme solution but supplemented with 300 μM Ca^{2+} and 1 mg/ml bovine serum albumin (BSA; Sigma-Aldrich, Bornem, Belgium). The solution was then filtered through a nylon mesh (250 μm) and centrifuged at 200 rpm for 2 min. The resulting pellet was washed with a Tyrode solution without enzymes containing 0.5 mM Ca^{2+} and BSA. The solution was left for decantation for 5–10 min, and the pellet was again washed with a Tyrode solution containing 1 mM Ca^{2+} and BSA. Myocytes thus obtained were kept at room temperature (21–23 °C) and used for experiments within 6–8 h.

VSMC isolation

Mice were anesthetized with CO_2 and then euthanized. Vascular smooth muscle cells (VSMC) were isolated according to a method previously described [29]. Mesenteric arteries were carefully dissected and cleaned of connective and endothelial tissues. Small pieces of mesenteric arteries were placed in a Ca^{2+}-free dissociation solution (SMDS) containing (in mM): NaCl 145, KCl 4.2, $MgCl_2$ 1.2, KH_2PO_4 0.6, HEPES 10, glucose 11, pH 7.4 (with NaOH), which was supplemented with 0.8 mg/ml papain (Worthington), 1 mg/ml BSA, and 1 mg/ml dithiothreitol (Sigma-Aldrich). These preparations were incubated at 37 °C for 10–12 min in a shaking water bath. After four or five washings in SMDS-10 μM Ca^{2+}, a second 10–12 min incubation was performed with SMDS containing 10 μM Ca^{2+}, 0.56 mg/ml collagenase F (Sigma-Aldrich), and 1 mg/ml BSA. Single cells were obtained by gentle trituration using a large-bore glass pipette stored in SMDS solution at 4 °C and used within the same day. Isolated VSMC were distinguished from other cells by their characteristic elongated shape. Only cells with a smooth birefringent membrane were used for recordings. VSMC were also characterized by immunocytochemistry using selective markers such as SM-alpha-actin and calponin (data not shown).

Patch-clamp recordings

Currents through the L-type Ca^{2+} channels were recorded at room temperature (21–23 °C) using the whole-cell configuration of the patch-clamp technique [18]. Ventricular cardiomyocytes (VCM) or VSMCs were placed directly in the recording chamber and let to settle for a few minutes before starting superfusion with the external solution. The composition of the extracellular solution for VCM was (in mM): NaCl 117, CsCl 20, $CaCl_2$ 2, $MgCl_2$ 1.8, HEPES 10, glucose 10, and pH 7.4. For VSMC, the extracellular solution contained NaCl 140, KCl 2.7, $BaCl_2$ 10, HEPES 10, glucose 10, and pH 7.4. The composition of the intracellular solution for VCM was (in mM): CsCl 130, $MgCl_2$ 2, $CaCl_2$ 4.7, EGTA 11, HEPES 10, Na_2ATP 5, Na_2GTP 0.4, Na_2-creatine phosphate 5, and pH 7.2 (free intracellular Ca^{2+} ~108 nM). For VSMC, the intracellular solution contained CsCl 130, $MgCl_2$ 2, HEPES 10, EGTA 10, Na_2ATP 4, and pH 7.2. Pipette resistances ranged from 1 to 1.2 MΩ for VCM and from 7 to 10 MΩ for VSMC.

Whole-cell currents in VCM were recorded using an RK-300 patch-clamp amplifier (Biologic). Currents were filtered at 3 KHz and were digitized at 20 KHz using a Labmaster DMA TL-1-125 (Mentor, Ohio, USA) and the ACQUIS1 software (CNRS License, France). In VSMC, currents were recorded using an Axopatch 200 patch-clamp amplifier (Molecular Devices, Sunnyvale, USA). Currents were filtered at 2 KHz and were digitized at 10 KHz using a Digidata 1322A driven by pClamp 10.2 software (Molecular Devices). L-type currents were routinely monitored at 0 mV using 300 ms (VCM) or 250 ms (VSMC) pulses from a holding potential (HP) of −80 mV. In VCM, a 50-ms prepulse to −40 mV was used to inactivate the fast Na^+ current. In spite of the fact that we have detected the expression of $Ca_V3.1$ and $Ca_V3.2$ mRNA in mesenteric VSMC (data not shown), we could never detect functional T-type Ca^{2+} currents in our cells using either kinetic or pharmacological analyses: We did not detect differences in the voltage-dependent Ca^{2+} currents (VDCC) elicited from a holding potential of −50 or −80 mV; the tail currents could always be fitted to a mono-exponential function and nifedipine (1 μM) blocked all the VDCC in our cells [38]. Ca^{2+} currents were measured as the difference between peak inward current and the current level at the end of the voltage-clamp pulse. Ba^{2+} currents were measured as the difference between peak current and the current recorded in the presence of Ca^{2+} at the end of the voltage-clamp pulse. Current-to-voltage (I-V) and availability curves were constructed using standard voltage-clamp protocols.

Potentials for half-maximal availability ($V_{0.5}$) and the slope factors (s) were obtained after fitting the experimental data with Boltzmann functions. Data analyses were performed with the softwares Clampfit (Molecular Devices), ACQUIS1, and Origin 7.5 (OriginLab Corporation, Northhaptom, USA). Results were analyzed using a Student's *t* test for paired or unpaired samples as required. Differences were considered statistically significant when $p<0.05$. Results are expressed as mean±standard error of the mean.

Results

Effects of CA on rat aorta and on isolated mouse heart

Here, we confirmed previous studies [39, 40] showing that CA relaxes endothelium-deprived rat aortic rings pre-contracted by KCl. In our experimental conditions, this occurred in a concentration-dependent manner (Fig. 1a, b) with an IC_{50} of 334±30 μM and a Hill number of 1.4±0.1. The maximal inhibition of aortic contraction (100 %) was attained at 3 mM.

As mentioned above, CA has been shown to have complex effects on isolated guinea pig cardiac preparations [20]. We found that CA exerts a modest but concentration-dependent negative inotropic effect in isolated mouse hearts. In paced hearts, a maximal decrease in contraction force of ~35 % was attained at the highest concentrations used at 1 and 3 mM (Fig. 1c). CA did not significantly affect the QRS duration and amplitude or the corrected QT interval (QTc) in spontaneously beating hearts at any of the studied concentrations. However, the RR interval showed a tendency to increase with CA concentration attaining significantly greater values at 1 and 3 mM (Fig. 1d; $p<0.05$). These findings prompted us to test the effects of CA on L-type Ca^{2+} channels in mouse cardiomyocytes and vascular smooth muscle cells.

Effects of CA on L-type Ca^{2+} current in VCM

In control condition, the mean I_{CaL} density (2 mM Ca^{2+} as charge carrier) at +10 mV in VCM was 6.9±0.6pF/pF (Cm= 200±9 pF; $n=33$). The inactivation phase of the currents was fitted by two exponentials yielding 9.4±0.8 and 63.5±4.0 ms for the fast (τ_{fast}) and slow (τ_{slow}) components, respectively. Extracellular perfusion with CA resulted in a pulse to pulse

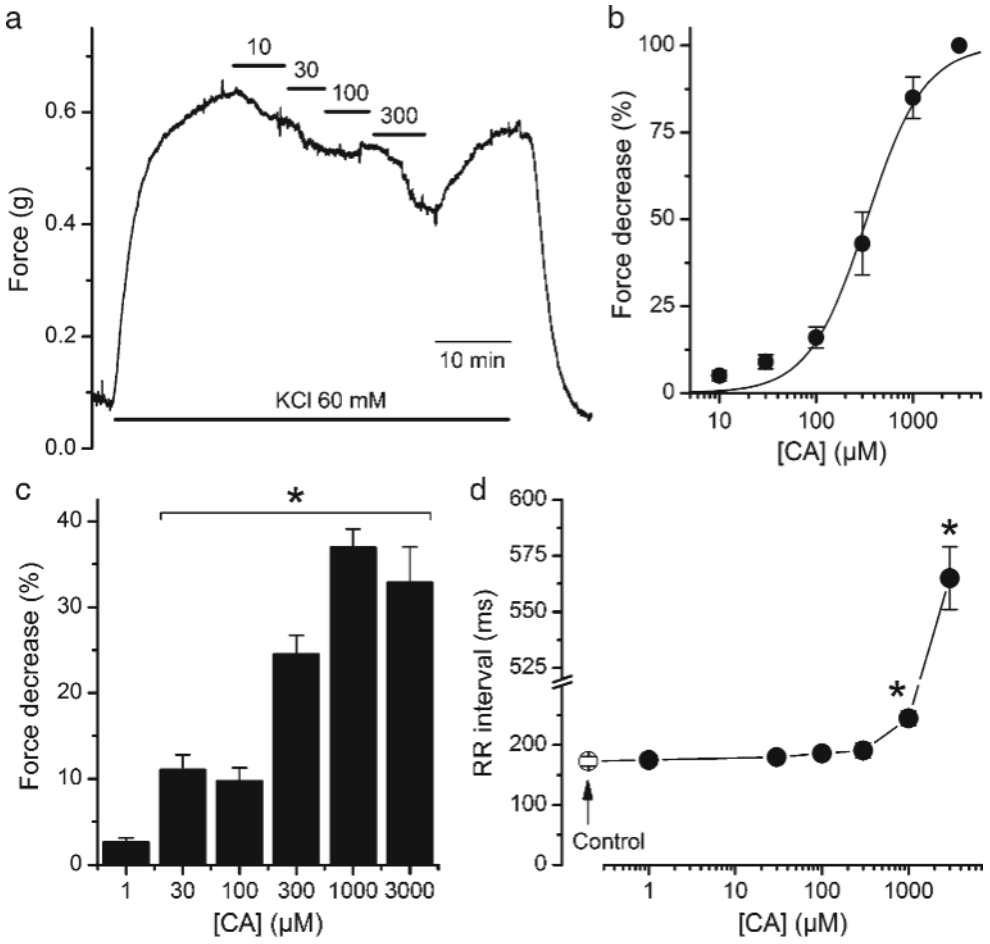

Fig. 1 Effects of CA on rat aortic rings and isolated mouse hearts. **a** Example of the vasorelaxing effect of CA at different concentrations in a rat aortic ring pre-contracted with 60 mM KCl. **b** Concentration-dependent vasorelaxing effect of CA ($n\geq4$). The *solid line* represents the fit with a Hill function. **c** Concentration-dependent negative inotropic effect of CA on isolated paced mice hearts ($n\geq5$). **d** Effect of CA on the RR interval. The *asterisks* denote statistically significant effects of CA with $p<0.05$

decrease of I_{CaL} that reached a steady state in ~1 min (Fig. 2a). The effects of CA were concentration-dependent, but reached a plateau at concentrations beyond ~1 μM (Fig. 2b, c). These effects were characterized by an IC_{50} of 0.07±0.02 μM, a Hill coefficient of 0.7±0.1 and a maximal inhibition of 70±2 % (Fig. 2c). CA caused a concentration-dependent decrease of the rate of I_{CaL} inactivation. This effect was characterized by a significant increase of both τ_{fast} and τ_{slow} at concentrations of 3 μM or higher (Fig. 2d, e).

The action of CA on I_{CaL} in VCM was barely voltage-dependent. There was no significant shift in the I-V curve even at the highest CA concentrations used (Fig. 3a, b). The potential for half-maximal availability ($V_{0.5}$) was only significantly shifted from −25.0±1.2 mV to −30.0±0.5 mV at 30 μM ($p<0.05$; Fig. 3c). Higher concentrations of CA resulted in similar changes in $V_{0.5}$. No changes were observed in the slope factor or on the I_{CaL} availability at positive prepulse potentials.

Effects of CA on L-type Ca^{2+} current in VSMC

Due to the low I_{CaL} density at normal extracellular Ca^{2+} concentrations (2 mM) in VSMC, we used 10 mM Ba^{2+} as a charge carrier. I_{BaL} was routinely monitored at 0 mV with 50-ms voltage-clamp pulses applied from a holding potential (HP) of −80 mV. Under these conditions, control I_{BaL} density was 3.5±0.4 pA/pF (Cm=17.7±1.4 pF, N=15). CA exerted a minor effect on I_{BaL} at 10 and 100 μM. However, at higher concentrations, CA induced a pulse to pulse decrease of I_{BaL} that reached a steady state in 1.5 to 2 min (Fig. 4a). This effect was reversible when taking into account the normal rundown of the L-type current in

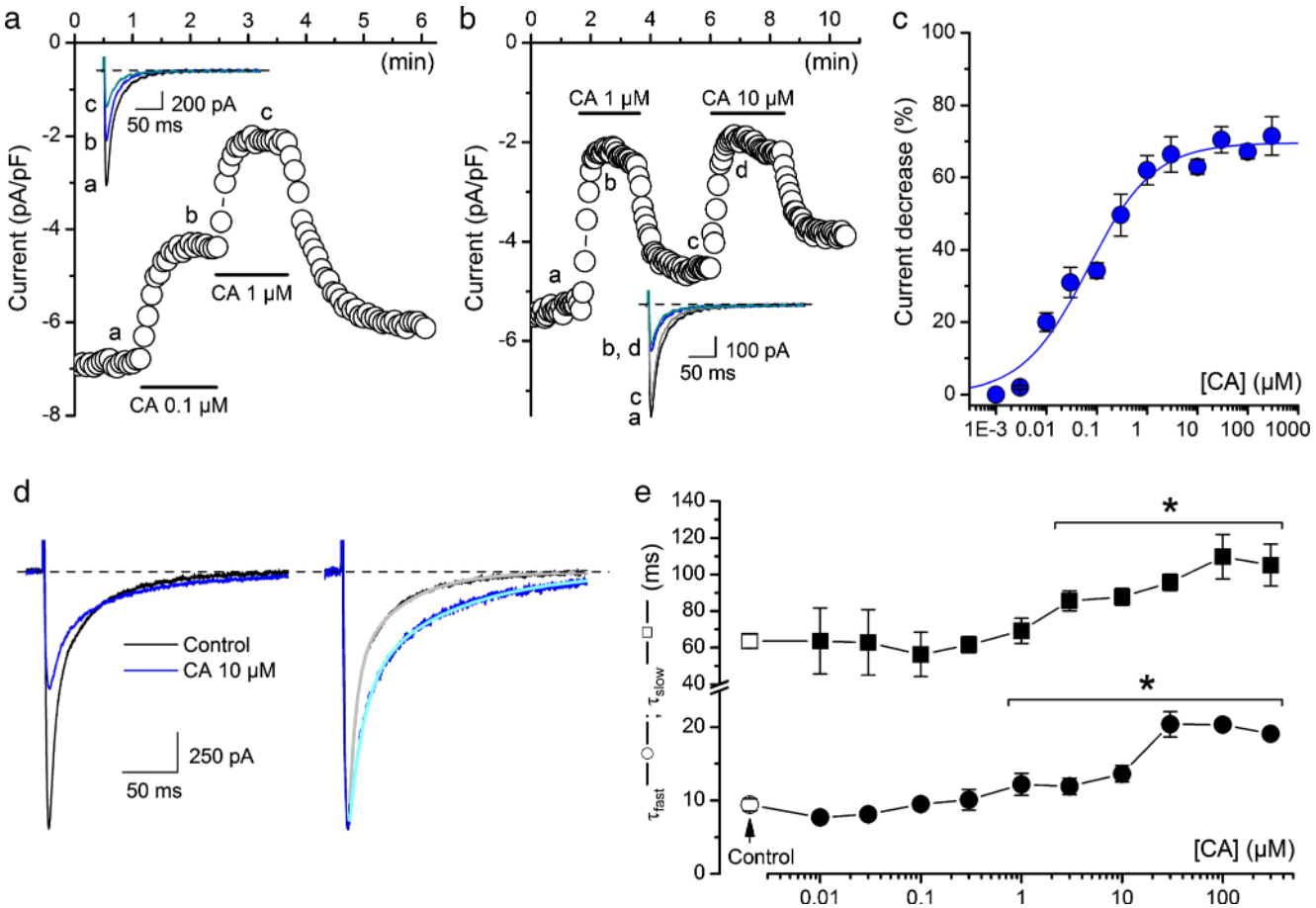

Fig. 2 Effects of CA on the L-type Ca^{2+} current in mouse ventricular cardiomyocytes. **a**, **b** Examples of the effects of extracellular application of CA at concentrations of 0.1, 1, and 10 μM on L-type Ca^{2+} currents recorded at +10 mV. The *insets* show the current traces corresponding to the time points indicated by the labels *a*, *b*, *c*, and *d*. Note that CA does not cause more inhibition at a concentration of 10 μM than at 1 μM. **c** Concentration-dependent decrease of I_{CaL} amplitude by CA in VCM ($n\geq 5$). The *solid line* corresponds to the fit by a Hill function. **d** *Left*: superposition of current traces recorded in control and during application of 10 μM CA. *Right*: normalized current traces demonstrating that CA slows down channel inactivation. The *solid lines* represent the fit of the inactivation phase of the current with a double-exponential function with fast and slow components. **e** Concentration-dependent effects of CA on the time constants of fast (τ_{fast}) and slow (τ_{slow}) inactivation of I_{CaL}. The *asterisks* denote statistically significant effects of CA ($p<0.05$) with respect to τ_{fast} and τ_{slow} obtained in control condition

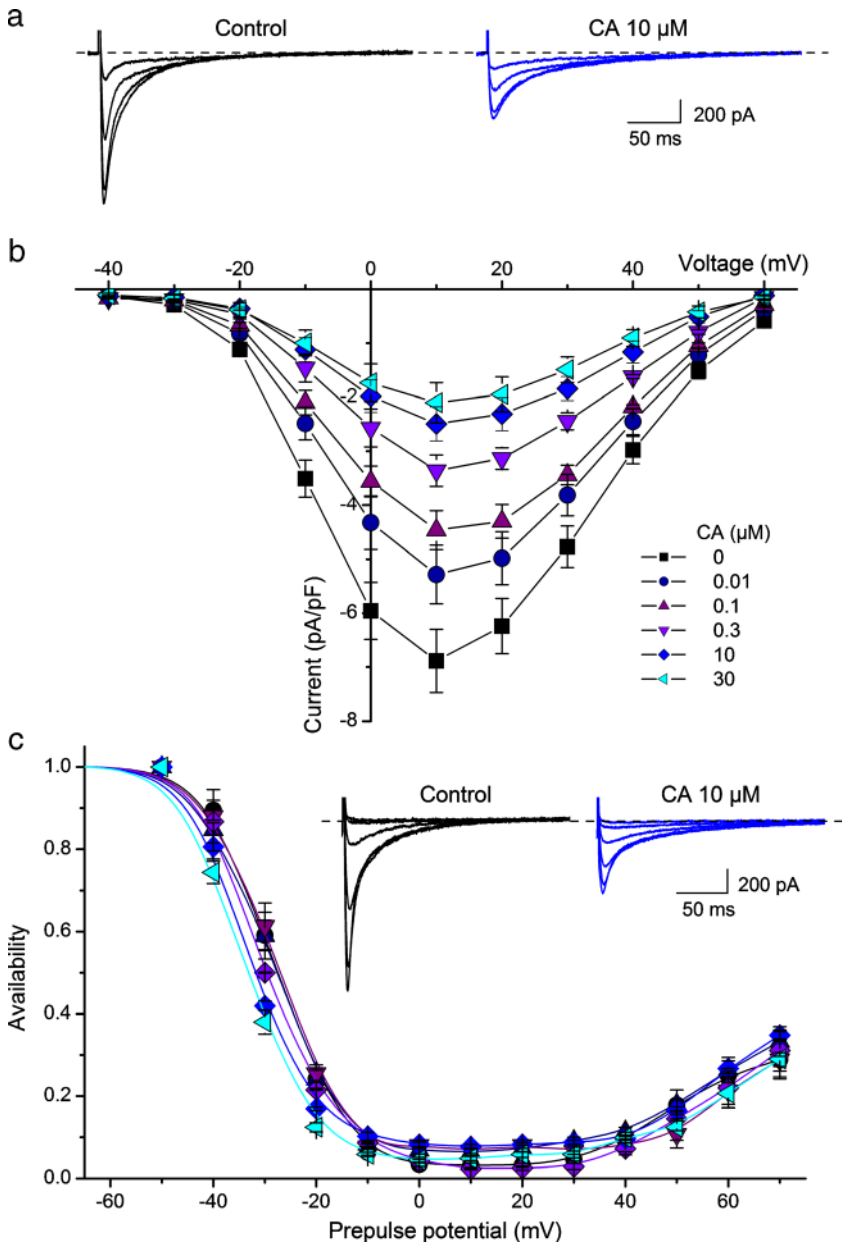

Fig. 3 Effects of CA on the voltage dependence of activation and inactivation of L-type Ca^{2+} currents in mouse ventricular cardiomyocytes. **a** Representative current traces recorded in the voltage range from −20 to + 10 mV in control and in the presence of 10 μM CA. **b** Concentration-dependent effect of CA on the current-voltage (I-V) relationship of I_{CaL}. Note that CA produced no shift on the I-V curve. **c** Availability curves of I_{CaL} obtained in control and the presence of CA at various concentrations (same legend as is panel **b**). VCM were clamped at a HP of −80 mV and a double-pulse voltage-clamp protocol was applied at a frequency of 0.125 Hz. A fixed 300-ms test pulse to +10 mV was preceded by 300-ms prepulses applied from −50 to +70 mV. A short 5-ms gap at the HP separated pre- and test pulses. I_{CaL} at each test pulse was normalized to maximal I_{CaL} and plotted against the prepulse potential. The *insets* show current traces recorded after prepulse potentials between −50 and −10 mV in control and in the presence of 10 μM CA

this preparation. The concentration-effect curve for the inhibitory action of CA on I_{BaL} was fit with a Hill function characterized by an IC_{50} of 0.81±0.02 mM, a Hill number of 2.2±0.13, and a maximal inhibition of 100 % (Fig. 4b).

To study the effects of CA on the inactivation kinetics of I_{BaL}, we applied 500-ms pulses to 0 mV (HP=−80 mV) every 30 s. The decrease in I_{BaL} by CA was accompanied by an acceleration of its inactivation kinetics (Fig. 4c, d). As observed in VCM, CA did not cause significant changes in the shape of the I-V curves recorded in VSMC (Fig. 5a, b). In contrast, at 1 mM concentration, CA significantly shifted the potential for half-maximal availability ($V_{0.5}$) from a control value of −21.8±4.5 mV to −40.6± 3.4 mV ($p<0.05$; Fig. 5c). All the effects of CA on the biophysical properties of I_{BaL} were readily reversed upon washout.

The action of CA on L-type currents is affected by the charge carrier

The effects of CA on the L-type currents in both VCM and VSMC were significantly different. First, CA was less potent and effective in decreasing I_{BaL} in VSMC than I_{CaL} in VCM, and second, CA accelerated I_{BaL} inactivation in VSMC and slowed down inactivation in VCM. Since $Ca_V1.2$ channel is

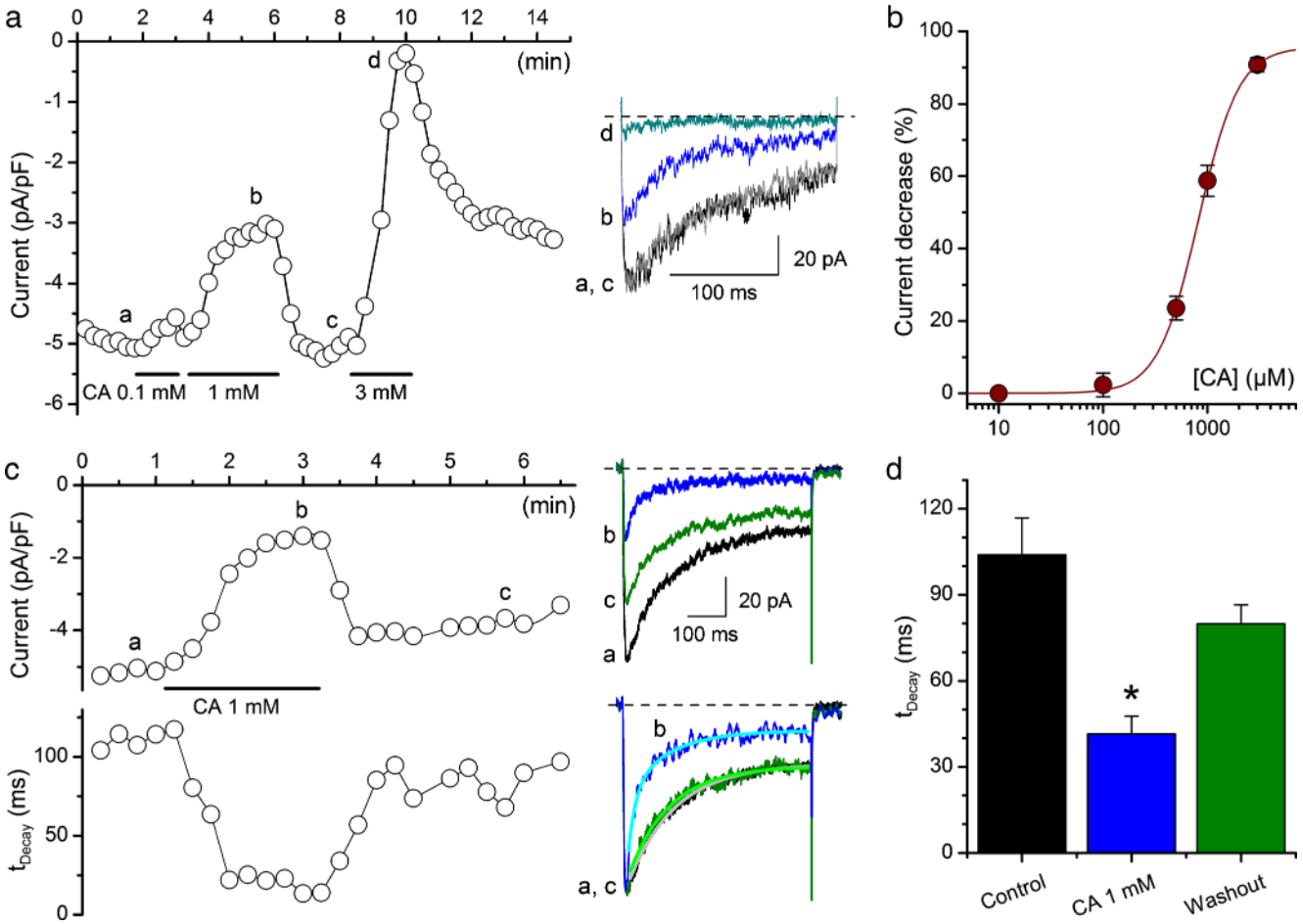

Fig. 4 Effects of CA on the L-type Ba^{2+} current in vascular smooth muscle cells. **a** Example of the effects of extracellular application of CA at concentrations of 0.1, 1, and 3 mM on L-type Ba^{2+} currents recorded at 0 mV. Note that CA effect was largely reversible. The current traces shown in the inset correspond to control condition (labels *a* and *c*) and two concentrations of CA (labels *b*, 1 mM, and *d*, 3 mM). **b** Concentration-dependent decrease of I_{BaL} amplitude by CA in VSMC ($n \geq 5$). The *solid line* corresponds to the fit by a Hill function. **c** Time course of the effect of 1 mM CA on current density and time for 50 % inactivation (t_{Decay}). The *upper inset* shows current traces at the times indicated by the labels *a*, *b*, and *c*. The *bottom inset* shows normalized current traces demonstrating that CA accelerates channel inactivation. The *solid lines* represent the fit of the inactivation phase of the current with a single- (traces labeled with *a* and *c*) or double-exponential function (trace labeled with *b*). **d** Effects of 1 mM CA on t_{Decay} of I_{BaL} ($n=5$). The *asterisk* denotes statistically significant difference ($p<0.05$) between the values obtained in the presence of 1 mM CA and those obtained in control condition and after washout

similarly expressed in both VSMC and VCM, a possible reason for the different effects could be the permeant cation used in each cell preparation. We, thus, performed experiments in VCM substituting Ba^{2+} for Ca^{2+} as charge carrier. The results show that CA reversibly inhibited I_{BaL} in a pulse to pulse manner (Fig. 6a), but with an IC_{50} of 37.3±2.4 μM (Fig 6b; ~3 orders of magnitude less potent than in Ca^{2+}), a Hill number of 1.4±0.1 and a maximal inhibition of 84± 1.5 %. Interestingly, CA decreased the inactivation time constant of I_{BaL} in a dose-dependent manner (Fig. 6c), as shown above for VSMC. These results suggest that not only the potency of CA but also its effect on the inactivation time course of the current through the $Ca_V1.2$ channel depend on the charge carrier.

Discussion

As early as 1975, Harada and Yano suggested that part of the beneficial effects of cinnamon in traditional medicine could be related to a peripheral vasodilating action [20]. They indeed showed that CA decreases arterial blood pressure by inducing peripheral vasodilation, but no mechanisms could be proposed at that time. The identification of TRPA1 as a very sensitive target of cinnamaldehyde in nociceptive neurons [6] raised the possibility of a nerve-evoked vasodilation mechanism involving TRPA1 activation. Indeed, Bautista et al. [7] proposed that activation of TRPA1 channels in sensory nerve endings causes Ca^{2+} influx and release of CGRP, which binds to its G protein-coupled receptor on the plasma membrane of

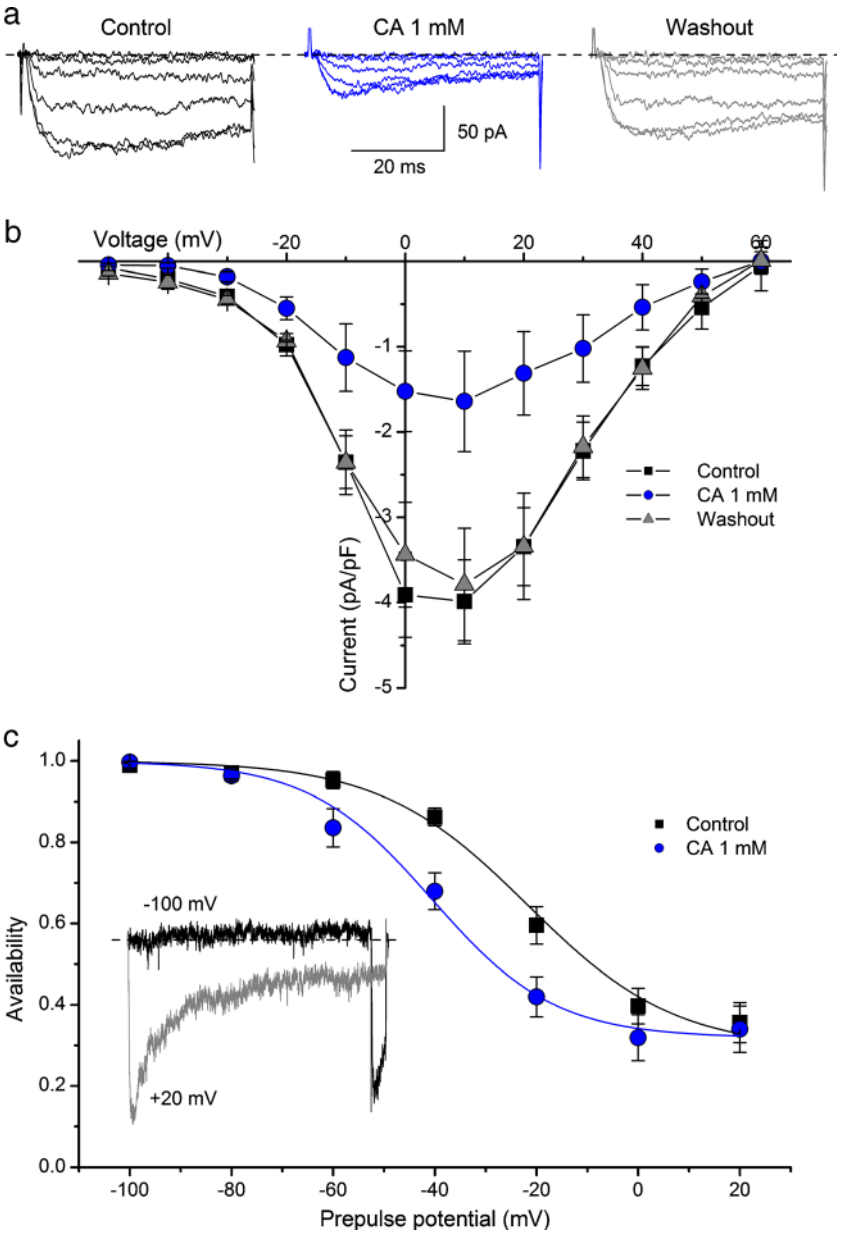

Fig. 5 Effects of CA on the voltage-dependence of activation and inactivation of L-type Ba^{2+} currents in mouse vascular smooth muscle cells. **a** Representative effects of 1 mM CA on I_{BaL} traces recorded in the voltage range from −40 to + 10 mV. **b** Effect of 1 mM CA on current-to-voltage (I-V) relationship of I_{BaL}. Note that CA produced no shift on the I-V curve. **c** Availability curves of I_{BaL} obtained in control and the presence of 1 mM CA. VSMC were clamped at a HP of −100 mV and a double-pulse voltage-clamp protocol was applied: a fixed 50-ms test pulse to 0 mV was preceded by 500-ms prepulses applied from −50 to + 20 mV. I_{BaL} at each test pulse was normalized to maximal I_{BaL} and plotted against prepulse potential. The *inset* shows examples of current traces corresponding to prepulses to −100 and +20 mV in control condition

vascular smooth muscle cells to cause membrane hyperpolarization and myocyte relaxation. The involvement of the TRPA1/CGRP pathway in vasodilation was supported by the results of Graepel et al. [16] and Kunkler et al. [24], showing that TRPA1 activation by CA, 4-ONE, or allyl isothiocyanate stimulated the release of CGRP and induce vasodilation. In addition, activation of TRPA1 and the consequent Ca^{2+} influx in endothelial cells may lead to smooth muscle cell relaxation and vasodilation [12, 13, 35]. Interestingly, Pozsgai et al. found that CA can dilate pre-contracted mouse mesenteric artery rings in an endothelium-independent manner, but genetic ablation of *Trpa1* failed to fully abrogate CA effects [34]. These results indicate that CA action on the vasculature is more complex and involves component(s) independent from the TRPA1 pathway.

Previous studies of El-Bassossy et al. [14, 40] had suggested the possibility of an inhibitory action on Ca^{2+} influx. This idea was supported by Xue et al. [39] who showed that CA exerted a vasodilatory action in rat aorta that was independent of endothelium and proposed that CA could be inhibiting Ca^{2+} influx and/or intracellular Ca^{2+}-release mechanisms. Although it is difficult to compare IC_{50}s due to different preparations and different experimental approaches, our results confirm the previous ones by showing that CA relaxes endothelium-deprived rat aortic rings pre-contracted with KCl in our case with an IC_{50} of ~330 μM. Without any

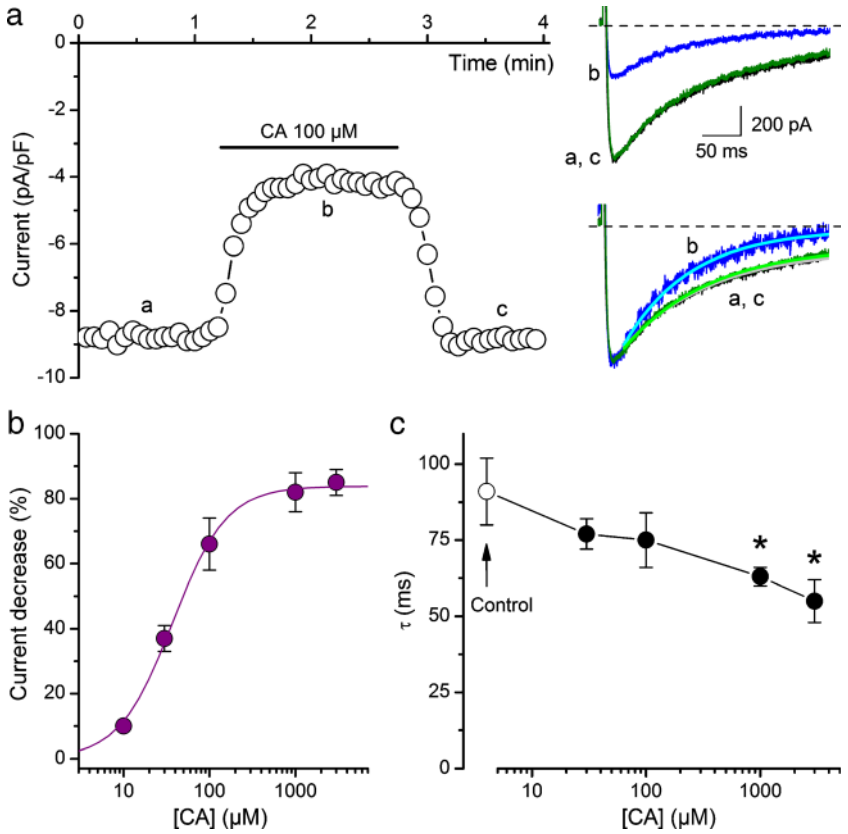

Fig. 6 Effects of CA on the L-type Ba^{2+} current in ventricular cardiomyocytes. **a** Time course of the effect of 100 μM CA on I_{BaL} in a VCM. Recording performed in 2 mM extracellular Ba^{2+}. The *upper inset* on the right shows current traces at the corresponding times (labels *a*, *b*, and *c*). The *lower inset* on the right shows normalized current traces demonstrating that CA accelerates channel inactivation. The *solid lines* represent the fit of the inactivation phase of the currents with single exponential functions. **b** Concentration-dependent decrease of I_{BaL} amplitude by CA in VCM ($n \geq 4$). The *solid line* corresponds to the fit by a Hill function. **c** Effect of different concentrations of CA on the inactivation time constant of I_{BaL}. Note that contrary to the findings with Ca^{2+} as charge carrier, CA decreases the inactivation time constant ($n \geq 4$). The *asterisks* denote statistically significant difference ($p<0.05$) between the values obtained in the presence of 1 and 3 mM CA and that obtained in control condition

direct evidence of TRPA1-functional expression in smooth muscle cells [12], a direct action of CA on Ca^{2+} influx (or intracellular Ca^{2+}-release mechanisms) seems to be the most plausible explanation.

Here, we show for the first time that CA inhibits I_{CaL} in both cardiac and vascular smooth muscle cells. Inhibition of I_{CaL} by CA in VCM and VSMC was concentration-dependent and was achieved in a pulse to pulse manner, an action which is similar to that of the classic phenylalkylamine Ca^{2+} channel blocker verapamil [37]. However, differences in current inhibition were observed between VCM and VSMC. First, although CA was concentration-dependent in both cell types, its action was very potent in VCM (with an IC_{50} of 0.07 μM and maximal inhibition of ~70 %) in deep contrast with VSMC in which the IC_{50} was ~0.8 mM but with a maximal inhibition of ~100 %. Second, in VCM, the effect was mildly voltage-dependent. Maximal hyperpolarizing shift of availability curve was ~5 mV at 30 μM or higher concentrations. In VSMC, the hyperpolarizing shift was ~20 mV (1 mM CA). Third, in VCM, the inhibition of I_{CaL} was accompanied by an increase in inactivation time constants with maximal increases (at 30 μM and over) for τ_{fast} and τ_{slow} of about 10 and 50 ms, but in VSMC, the time for 50 % inactivation was decreased by about 20 ms by CA (1–3 mM). Since the $Ca_V1.2$ channel is equally expressed in both VCM and VSMC, a plausible explanation for these discrepancies could be the use of 10 mM Ba^{2+} as charge carrier in VSMC. It has been previously shown that the permeant cation can influence block of high threshold Ca^{2+} channels. For instance, Carbone and Lux found that ω-conotoxin blockade could distinguish between Ca^{2+}- and Na^{+}-permeable states of neuronal Ca^{2+} channels [9]. These authors proposed that the two permeability states of the channels correspond to conformations with different sensitivities to blockers. This idea was also supported by the facts that the effects of protons [33] and dihydropyridines [22] on the cardiac L-type Ca^{2+} channel are dependent on the permeant ion. We tested whether the nature of the charge carrier could influence CA effects by performing experiments in VCM using Ba^{2+} as

the permeant ion. We found that the inhibition was ~3 orders of magnitude less potent and more effective than in the presence of Ca^{2+} and that CA increased the rate of inactivation of I_{BaL}, thus resembling to the results obtained in VSCM.

However, at this point, we cannot discard the distinct subunit composition of L-type Ca^{2+} channels in VCM and VSMC as alternative explanation for the differences CA effects. $Ca_V1.2$ is the pore-forming subunit in both cell types, but it has been reported that alternative splicing occurs in VSMC, resulting in different current kinetics [11]. Moreover, the accessory subunit composition of L-type Ca^{2+} channels in VSMC is known to influence the current kinetics and the response to channel modulators [38]. Future experiments may help to determine whether CA effects are determined by the different conduction and/or gating properties observed in the presence of Ca^{2+} and Ba^{2+}.

The inhibition of L-type Ca^{2+} channels in VCM can readily explain the negative inotropic effect, and part of the negative chronotropic effect, we found in isolated mouse hearts. Interestingly, CA was only modestly effective in reducing the cardiac contractility, with a maximal inhibition of ~35 %. This could be explained by the inability of CA to fully inhibit the L-type Ca^{2+} current in VCM. On the other hand, we found that CA induced complete arterial relaxation in agreement with previous reports [34, 39, 40]. However, it remains difficult to understand how some specific features of CA actions on L-type Ca^{2+} currents (potent but incomplete inhibition) and TRPA1 channels (induction of dynamic changes in Ca^{2+} permeability [10, 21] and bimodal effect [4]) impact on the function of intact arteries. Moreover, we cannot discard that CA acts on other contractility regulators. Due to the lack of pharmacokinetic studies on cinnamaldehyde in humans, it is also not possible to precise at this point to what extent the actions of CA on $Ca_V1.2$ and TRPA1 channels may contribute to the reported effects of cinnamon on blood pressure.

On the other hand, our results do lead to the conclusion that TRPA1 should not be considered as a specific target of CA in the cardiovascular system (see also [26]). Moreover, they raise the possibility that the inhibition of voltage-gated Ca^{2+} channels influences the chemosensory properties of CA. These elements have significant implications, considering the very frequent use of this compound to probe the pathophysiological roles of TRPA1 [32]. Finally, our findings underscore the importance of testing the effects of TRP channel modulators on the "classical," but certainly still relevant, voltage-gated ion channels [27].

Acknowledgments Research was supported by Spanish public funds from Instituto de Salud Carlos III ISCIII-FEDER RD12/0042/0006 (Heracles Program), Spanish MINECO grant BFU2010-15898 (MTPG) and Junta de Castilla y León grant VA094A11-2 (JRLL), and grants from the Belgian Federal Government (IUAP P7/13), the Research Foundation-Flanders (Grant G.0765.13), and the Research Council of the KU Leuven (Grants GOA 2009/07 and PF-TRPLe).

References

1. Akilen R, Pimlott Z, Tsiami A, Robinson N (2013) Effect of short-term administration of cinnamon on blood pressure in patients with prediabetes and type 2 diabetes. Nutrition 29:1192–1196
2. Akilen R, Tsiami A, Devendra D, Robinson N (2010) Glycated haemoglobin and blood pressure-lowering effect of cinnamon in multi-ethnic type 2 diabetic patients in the UK: a randomized, placebo-controlled, double-blind clinical trial. Diabet Med 27: 1159–1167
3. Akilen R, Tsiami A, Devendra D, Robinson N (2012) Cinnamon in glycaemic control: systematic review and meta analysis. Clin Nutr 31:609–615
4. Alpizar YA, Gees M, Sanchez A, Apetrei A, Voets T, Nilius B, Talavera K (2013) Bimodal effects of cinnamaldehyde and camphor on mouse TRPA1. Pflugers Arch 465:853–864
5. Alvarez-Collazo J, Diaz-Garcia CM, Lopez-Medina AI, Vassort G, Alvarez JL (2013) Zinc modulation of basal and beta-adrenergically stimulated L-type Ca^{2+} current in rat ventricular cardiomyocytes: consequences in cardiac diseases. Pflugers Arch 464:459–470
6. Bandell M, Story GM, Hwang SW, Viswanath V, Eid SR, Petrus MJ, Earley TJ, Patapoutian A (2004) Noxious cold ion channel TRPA1 is activated by pungent compounds and bradykinin. Neuron 41:849–857
7. Bautista DM, Movahed P, Hinman A, Axelsson HE, Sterner O, Hogestatt ED, Julius D, Jordt SE, Zygmunt PM (2005) Pungent products from garlic activate the sensory ion channel TRPA1. Proc Natl Acad Sci U S A 102:12248–12252
8. Bers DM (2002) Cardiac excitation-contraction coupling. Nature 415:198–205
9. Carbone E, Lux HD (1988) Omega-conotoxin blockade distinguishes Ca from Na permeable states in neuronal calcium channels. Pflugers Arch 413:14–22
10. Chen J, Kim D, Bianchi BR, Cavanaugh EJ, Faltynek CR, Kym PR, Reilly RM (2009) Pore dilation occurs in TRPA1 but not in TRPM8 channels. Mol Pain 5:3
11. Cheng X, Liu J, Asuncion-Chin M, Blaskova E, Bannister JP, Dopico AM, Jaggar JH (2007) A novel $Ca_V1.2$ N terminus expressed in smooth muscle cells of resistance size arteries modifies channel regulation by auxiliary subunits. J Biol Chem 282:29211–29221
12. Earley S (2012) TRPA1 channels in the vasculature. Br J Pharmacol 167:13–22
13. Earley S, Gonzales AL, Crnich R (2009) Endothelium-dependent cerebral artery dilation mediated by TRPA1 and Ca^{2+}-activated K^+ channels. Circ Res 104:987–994
14. El-Bassossy HM, Fahmy A, Badawy D (2011) Cinnamaldehyde protects from the hypertension associated with diabetes. Food Chem Toxicol 49:3007–3012
15. Galan L, Talavera K, Vassort G, Alvarez JL (1998) Characteristics of Ca^{2+} channel blockade by oxodipine and elgodipine in rat cardiomyocytes. Eur J Pharmacol 357:93–105
16. Graepel R, Fernandes ES, Aubdool AA, Andersson DA, Bevan S, Brain SD (2011) 4-oxo-2-nonenal (4-ONE): evidence of transient receptor potential ankyrin 1-dependent and -independent nociceptive and vasoactive responses in vivo. J Pharmacol Exp Ther 337:117–124
17. Gruenwald J, Freder J, Armbruester N (2012) Cinnamon and health. Crit Rev Food Sci Nutr 50:822–834
18. Hamill OP, Marty A, Neher E, Sakmann B, Sigworth FJ (1981) Improved patch-clamp techniques for high-resolution current recording from cells and cell-free membrane patches. Pflugers Arch 391: 85–100
19. Harada M, Saito A (1978) Pharmacological studies on Chinese cinnamon. IV. Effects of cinnamaldehyde on the isolated heart of guinea pigs and its catecholamine releasing effect from the adrenal gland of dogs. J Pharm Dyn 1:89–97

20. Harada M, Yano S (1975) Pharmacological studies on Chinese cinnamon. II. Effects of cinnamaldehyde on the cardiovascular and digestive systems. Chem Pharm Bull (Tokyo) 23:941–947
21. Karashima Y, Prenen J, Talavera K, Janssens A, Voets T, Nilius B (2010) Agonist-induced changes in Ca^{2+} permeation through the nociceptor cation channel TRPA1. Biophys J 98:773–783
22. Kass RS, Arena JP, Chin S (1991) Block of L-type calcium channels by charged dihydropyridines. Sensitivity to side of application and calcium. J Gen Physiol 98:63–75
23. Kleefstra N, Logtenberg SJ, Groenier KH, Bilo HJ (2011) Reply to Akilen et al. Effect of cinnamon on glycated haemoglobin and blood pressure. Diabet Med 28:380
24. Kunkler PE, Ballard CJ, Oxford GS, Hurley JH (2011) TRPA1 receptors mediate environmental irritant-induced meningeal vasodilatation. Pain 152:38–44
25. Leach MJ, Kumar S (2012) Cinnamon for diabetes mellitus. Cochrane Database Syst Rev. doi:10.1002/14651858.CD007170.pub2, Art No.: CD007170
26. Macpherson LJ, Hwang SW, Miyamoto T, Dubin AE, Patapoutian A, Story GM (2006) More than cool: promiscuous relationships of menthol and other sensory compounds. Mol Cell Neurosci 32:335–343
27. Meseguer VM, Denlinger BL, Talavera K (2011) Methodological considerations to understand the sensory function of TRP channels. Curr Pharm Biotechnol 12:3–11
28. Moosmang S, Schulla V, Welling A, Feil R, Feil S, Wegener JW, Hofmann F, Klugbauer N (2003) Dominant role of smooth muscle L-type calcium channel $Ca_V1.2$ for blood pressure regulation. EMBO J 22:6027–6034
29. Moreno-Dominguez A, Cidad P, Miguel-Velado E, Lopez-Lopez JR, Perez-Garcia MT (2009) De novo expression of $K_V6.3$ contributes to changes in vascular smooth muscle cell excitability in a hypertensive mice strain. J Physiol 587:625–640
30. Namer B, Seifert F, Handwerker HO, Maihofner C (2005) TRPA1 and TRPM8 activation in humans: effects of cinnamaldehyde and menthol. Neuroreport 16:955–959
31. Nilius B, Appendino G (2013) Spices: the savory and beneficial science of pungency. Rev Physiol Biochem Pharmacol 164:1–76
32. Nilius B, Appendino G, Owsianik G (2012) The transient receptor potential channel TRPA1: from gene to pathophysiology. Pflugers Arch 464:425–458
33. Pietrobon D, Prod'hom B, Hess P (1988) Conformational changes associated with ion permeation in L-type calcium channels. Nature 333:373–376
34. Pozsgai G, Bodkin JV, Graepel R, Bevan S, Andersson DA, Brain SD (2010) Evidence for the pathophysiological relevance of TRPA1 receptors in the cardiovascular system in vivo. Cardiovasc Res 87:760–768
35. Qian X, Francis M, Solodushko V, Earley S, Taylor MS (2013) Recruitment of dynamic endothelial Ca^{2+} signals by the TRPA1 channel activator AITC in rat cerebral arteries. Microcirculation 20:138–148
36. Ranasinghe P, Pigera S, Premakumara GS, Galappaththy P, Constantine GR, Katulanda P (2013) Medicinal properties of 'true' cinnamon (*Cinnamomum zeylanicum*): a systematic review. BMC Complement Altern Med 13:275
37. Rubio LS, Garrido G, Llanes L, Alvarez JL (1993) Effects of tetrandrine on Ca^{2+}- and Na^{+}-currents of single bullfrog cardiomyocytes. J Mol Cell Cardiol 25:801–813
38. Tajada S, Cidad P, Colinas O, Santana LF, Lopez-Lopez JR, Perez-Garcia MT (2013) Down-regulation of $Ca_V1.2$ channels during hypertension: how fewer $Ca_V1.2$ channels allow more Ca^{2+} into hypertensive arterial smooth muscle. J Physiol 591:6175–6191
39. Xue YL, Shi HX, Murad F, Bian K (2011) Vasodilatory effects of cinnamaldehyde and its mechanism of action in the rat aorta. Vasc Health Risk Manag 7:273–280
40. Yanaga A, Goto H, Nakagawa T, Hikiami H, Shibahara N, Shimada Y (2006) Cinnamaldehyde induces endothelium-dependent and -independent vasorelaxant action on isolated rat aorta. Biol Pharm Bull 29:2415–2418
41. Zhang J, Berra-Romani R, Sinnegger-Brauns MJ, Striessnig J, Blaustein MP, Matteson DR (2007) Role of $Ca_V1.2$ L-type Ca^{2+} channels in vascular tone: effects of nifedipine and Mg^{2+}. Am J Physiol Heart Circ Physiol 292:H415–H425